New Numerical Technologies for the Simulation of Arc Welding Processes

Michel Bellet, Makhlouf Hamide, Christel Pequet, Patrice Lasne

Proc. MCWASP XII, 12th Int. Conf. on Modeling of Casting, Welding and Advanced Solidification Processes, Vancouver & Alaska, June 7-13, 2009, S. Cockcroft, D. Maijer (eds.), The Minerals, Metals & Materials Society, Warrendale, Pennsylvania, USA (2009) 563-570

NEW NUMERICAL TECHNOLOGIES FOR THE SIMULATION OF ARC WELDING PROCESSES

Michel Bellet [1], Makhlouf Hamide [1], Christel Pequet [2], Patrice Lasne [2]

[1] Mines ParisTech, CEMEF – Centre de Mise en Forme des Matériaux, CNRS UMR 7635, Sophia Antipolis, France; michel.bellet@mines-paristech.fr
[2] Transvalor SA, Sophia Antipolis, France; soudage@transvalor.com

Keywords: welding, finite elements, material deposit, adaptive meshing, inverse method

Abstract

The paper presents the main concepts of a newly-developed numerical code for arc welding simulation and analysis. The new numerical technologies essentially consist first of original methods for the modeling of material deposit allowing a direct simulation of joint formation, instead of usual element birth techniques. Second, a dynamic mesh optimization procedure, allowing error control. And third, a multivariable finite element inverse method for identification of heat sources.

Introduction

Numerical modelling plays an increasing part in the design and the optimization of welding processes and welded assemblies. The main objectives of such simulations are:

- To predict the geometry of the welded assembly, including weld bead shape.
- To follow the thermal and mechanical evolutions in the weld bead and in the part as well as the structural transformations and to evaluate the risks of defects during the process and in the final assembly.
- To predict the final mechanical properties of the assembly, starting from the prediction of residual stresses and structural variables.

Given those objectives, Transvalor and Cemef have developed a coupled finite element three-dimensional model for steel arc welding processes, named TRANSWELD. It is based on coupled solutions of heat transfer, metallurgical kinetics and mechanics. The interested reader is invited to refer to the following references regarding the coupled thermal-metallurgical-mechanical model, which will not be presented here [1-3].

The present paper addresses three issues that often constitute bottlenecks for the finite element simulation of welding processes, namely:

- Modelling of material deposit (filler material),
- Control of the mesh,
- Inverse modelling for identification of thermal sources.

Modelling of Material Deposit

In the literature, two classic methods can be found: the "quiet element" method and the "inactive element" or "element birth" method [4]. In those approaches, the metal supply is modelled by progressive activation of the finite elements that constitute the weld bead. Therefore, they suffer from three major defects:

- The geometry of the weld bead is defined *a priori* and does not result from the solution of the coupled physical phenomena governing the process;
- This is a very painful and time consuming task for the code user, especially for multipass simulation, for which each of the deposit layers must consist of a set of finite elements;
- This generally impedes dynamic remeshing during process simulation (see next Section).

In this paper, an alternative approach is presented in which the metal deposit is modelled in a more physical way with less constraint for the user. In practice (gas metal arc welding – GMAW), depending on the selection of adequate welding parameters, droplets of filler material, of variable size and arising from the fusion of the electrode, fall down into the weld pool after a flight through the electric arc. The partial and progressive solidification of the weld pool gives birth to the weld joint. Consequently, the material supply may be modelled by a source term in the mass conservation equation, for a selection of finite elements located in the fusion zone. For this purpose, a virtual cone is attached to the electrode tip and moves with it (Figure 1). An additional source term is then considered in elements that are in the liquid state and located in this cone (in red on the figure). The contribution of such an element K to the weak form of the mass conservation is then expressed by:

$$\int_K q\left(\nabla\cdot\mathbf{v}+\frac{1}{\rho}\frac{\mathrm{d}\rho}{\mathrm{d}t}-\bar{\dot{\theta}}\right)\mathrm{d}V \tag{1}$$

where $\mathbf{v}$ denotes the velocity field, ρ the density, q a test function, and $\bar{\dot{\theta}}=\dot{Q}/\sum_K V^K$ is an additional term standing for the average volumetric change rate [s^{-1}], $\dot{Q}$ [m^3/s] being the effective flow rate of filler material and V^K the volume of each selected element K. The bulging of the selected elements induces an evolution of the surface of the weld pool, which finally gives birth, after complete solidification, to the shape of the weld joint.

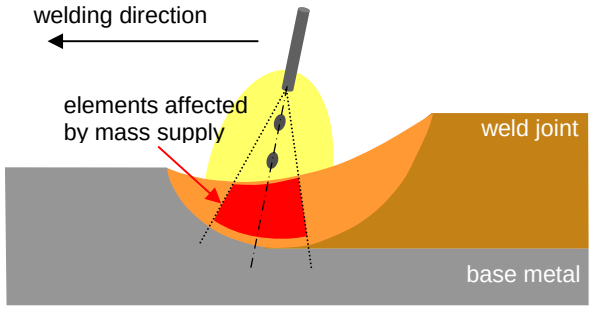

Figure 1. Schematics for the modelling of material deposit in GMA welding.

Two different numerical approaches can be distinguished: the Lagrangian method, in which the weld pool surface is represented by the boundary of the computational domain, and the interface tracking method, in which the position of the metal/air interface is estimated on a fixed background mesh. Those two methods are presented and discussed hereunder.

Lagrangian Method

This method consists in updating the mesh, and accordingly its boundary, at each time step according to the calculated velocity field. This velocity field results from the concurrent solution of momentum and mass conservation, using a velocity-pressure formulation [1, 15]. The updating scheme is:

$$^{t+\Delta t}\mathbf{x}={}^{t}\mathbf{x}+\Delta t\,\mathbf{v} \tag{2}$$

Despite several advantages (direct prescription of boundary conditions at the interface, no uncertainty in the evaluation of physical properties close to the interface, no numerical diffusion), this method has a major drawback. It may lead to intercontact between evolving joint surfaces in some particular situations (deposit in grooves, corners…).

Interface Tracking Method

In this method, the thermal-mechanical problem is solved on an extended domain, including a region in which the bead is supposed to form. This domain extension must then be neither too large (in order to limit the total number of dofs), neither too limited (as it should encompass the entirety of the formed joint). The metal/air discontinuity is then replaced by a transition region in which the tracking of the interface is achieved by means of the characteristic function α associated to metal (α value is 1 in the metal and 0 in the air). In the literature, the function α and the interface tracking method are often named "volume of fluid" and VOF method, respectively. This characteristic function α is of P0-type (that is constant on each element). It is used to apply a linear mixing rule to the thermophysical and mechanical properties. For instance, the stress deviator **s** and the density ρ appearing in the velocity-pressure mechanical problem are expressed in each element as:

$$\mathbf{s} = \alpha \mathbf{s}_m + (1-\alpha)\mathbf{s}_a \qquad \rho = \alpha \rho_m + (1-\alpha)\rho_a \tag{3}$$

where indices *m* and *a* denote metal and air, respectively. In this method, air is assumed to behave as a compressible medium, of compressibility modulus χ_a. The mass conservation equation on the extended domain Ω is then obtained by a mixing law, as follows:

$$\forall q \quad \int_\Omega q\left[\alpha\left(\nabla\cdot\mathbf{v} + \frac{1}{\rho_m}\frac{\mathrm{d}\rho_m}{\mathrm{d}t} - \dot{\bar{\theta}}\right) + (1-\alpha)(\nabla\cdot\mathbf{v} + \chi_a p)\right]\mathrm{d}V = 0 \tag{4}$$

Similar mixing rules are used when solving the thermal problem. Once the mechanical problem is solved, the new position of the interface is calculated by solving the following transport equation,

$$\frac{\partial_{msh}\alpha}{\partial t} + (\mathbf{v} - \mathbf{v}_{msh})\cdot\nabla\alpha = 0 \tag{5}$$

in which $\partial_{msh}/\partial t$ denotes time derivation with respect to the mesh, and $\mathbf{v}_{msh}$ the mesh velocity. The solution of this equation is achieved by a discontinuous Taylor-Galerkin method [5]. These methods have been implemented in the object-oriented C++ library Cimlib of Cemef [6].

Surface Tension

Surface tension and arc pressure have a strong influence on the shape of the weld pool surface. Hereunder is presented a method to take into account those effects. The presentation is done in the framework of the Lagrangian method. The extension to the interface tracking method will be done in the future. Locally, neglecting the tangential contribution arising from the Marangoni effect, the surface force **T** at the bath surface can be expressed as follows,

$$\mathbf{T} = \boldsymbol{\sigma}\mathbf{n} = -P_{arc}\mathbf{n} - \gamma\kappa\mathbf{n} \tag{6}$$

γ denoting the surface tension, κ the mean curvature (positive if convex, negative if concave) and **n** the outward unit normal vector. The associated contribution in the weak form of momentum conservation writes:

$$-\int_\Gamma \mathbf{T}\cdot\mathbf{v}^*\,\mathrm{d}S = \int_\Gamma P_{arc}\mathbf{n}\cdot\mathbf{v}^*\,\mathrm{d}S + \int_\Gamma \gamma\kappa\mathbf{n}\cdot\mathbf{v}^*\,\mathrm{d}S \tag{7}$$

The tangent gradient operator is then introduced, which is defined for a scalar field *f* by:

$$\underline{\nabla} f = \nabla f - (\mathbf{n}\cdot\nabla f)\cdot\mathbf{n} \tag{8}$$

The mean curvature is defined by [7]:

$$\kappa = \underline{\nabla}\cdot\mathbf{n} \tag{9}$$

A first formulation for the contribution (7) consists in directly replacing κ by its expression (9) [8]. But, (7) being expressed on the increment start configuration, this explicit expression has a limited stability. Now, introducing the Laplace-Beltrami operator, defined by:

$$\underline{\underline{\Delta}} f = \underline{\nabla} \cdot (\underline{\nabla} f) \tag{10}$$

it is possible to have access to the curvature vector along the boundary Γ [9]:

$$\underline{\underline{\Delta}} \mathbf{x} = \underline{\nabla} \cdot (\underline{\nabla} \mathbf{x}) = \kappa \mathbf{n} \tag{11}$$

Injecting this expression in (7), and integrating the last term by parts, we get:

$$\int_\Gamma \gamma \kappa \mathbf{n} \cdot \mathbf{v}^* \, \mathrm{d}S = -\int_{\partial\Gamma} \gamma \partial_\Gamma \mathbf{x} \cdot \mathbf{v}^* \, \mathrm{d}l + \int_\Gamma \gamma \underline{\nabla} \mathbf{x} : \underline{\nabla} \mathbf{v}^* \, \mathrm{d}S \tag{12}$$

Like Hysing [10], we neglect the contour integral. In the second integral, we can either consider nodal positions at the start of the time increment, or construct a semi-implicit form using the unknown velocity field **v** (to be calculated for the considered time step). Then, we get:

$$\int_\Gamma \gamma \kappa \mathbf{n} \cdot \mathbf{v}^* \, \mathrm{d}S = \int_\Gamma \gamma \underline{\nabla} ({}^t\mathbf{x}) : \underline{\nabla} \mathbf{v}^* \, \mathrm{d}S + \int_\Gamma \gamma \Delta t \underline{\nabla} \mathbf{v} : \underline{\nabla} \mathbf{v}^* \, \mathrm{d}S \tag{13}$$

The second term being symmetric positive definite, this yields an improved stability.

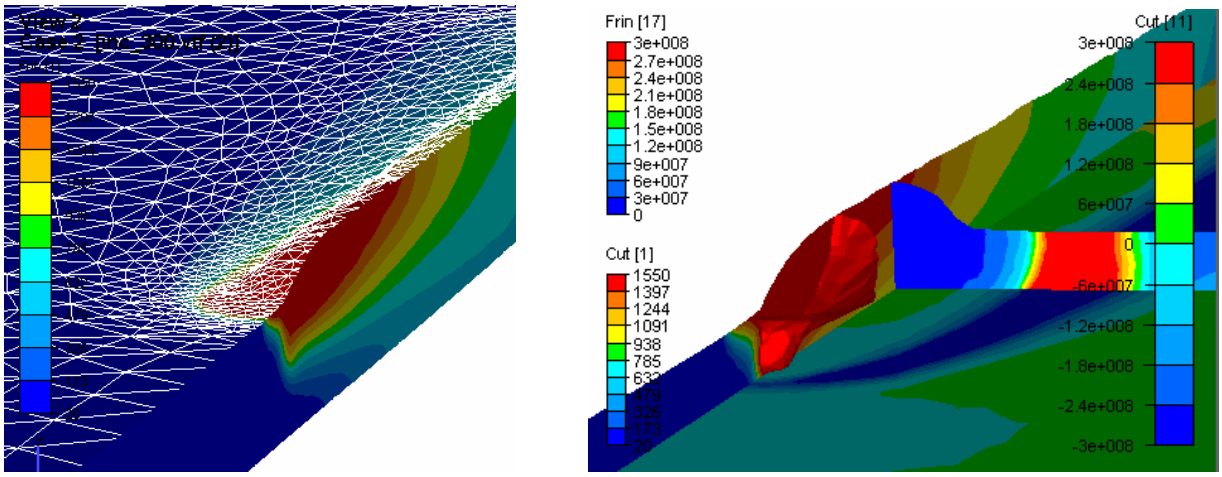

Figure 2. Modelling of a GMA welding (steel deposit on a steel plate), using the Lagrangian formulation. On the left, the formation of the bead can be seen, together with temperature distribution and adapted finite element mesh (see next Section). On the right, the iso-surface T_{solidus} shows the shape of the fusion zone. In the plane orthogonal to the bead is mapped the von Mises stress, while the axial stress component is mapped onto the horizontal section plane.

The two formulations (Lagrangian and VOF-type interface tracking) have been compared in terms of thermomechanical predictions. As shown in Figure 3, the shape of the weld joint, the temperature and stress distributions predicted by the two methods are in good agreement. The difference comes from a slightly different way of treating the heat transfer boundary conditions in the vicinity of the weld joint. This minor point should be fixed by future work.

Control of Finite Element Mesh

Given the steep gradients generated by welding processes, mesh control is indispensable in terms of results reliability. Following Fortin [11], it is assumed here that the interpolation error can serve as a good indicator for mesh adaptivity. Considering a P1 finite element discretization of a scalar field u, this interpolation error can be upper-bounded in each element K by the formula [12, 13]:

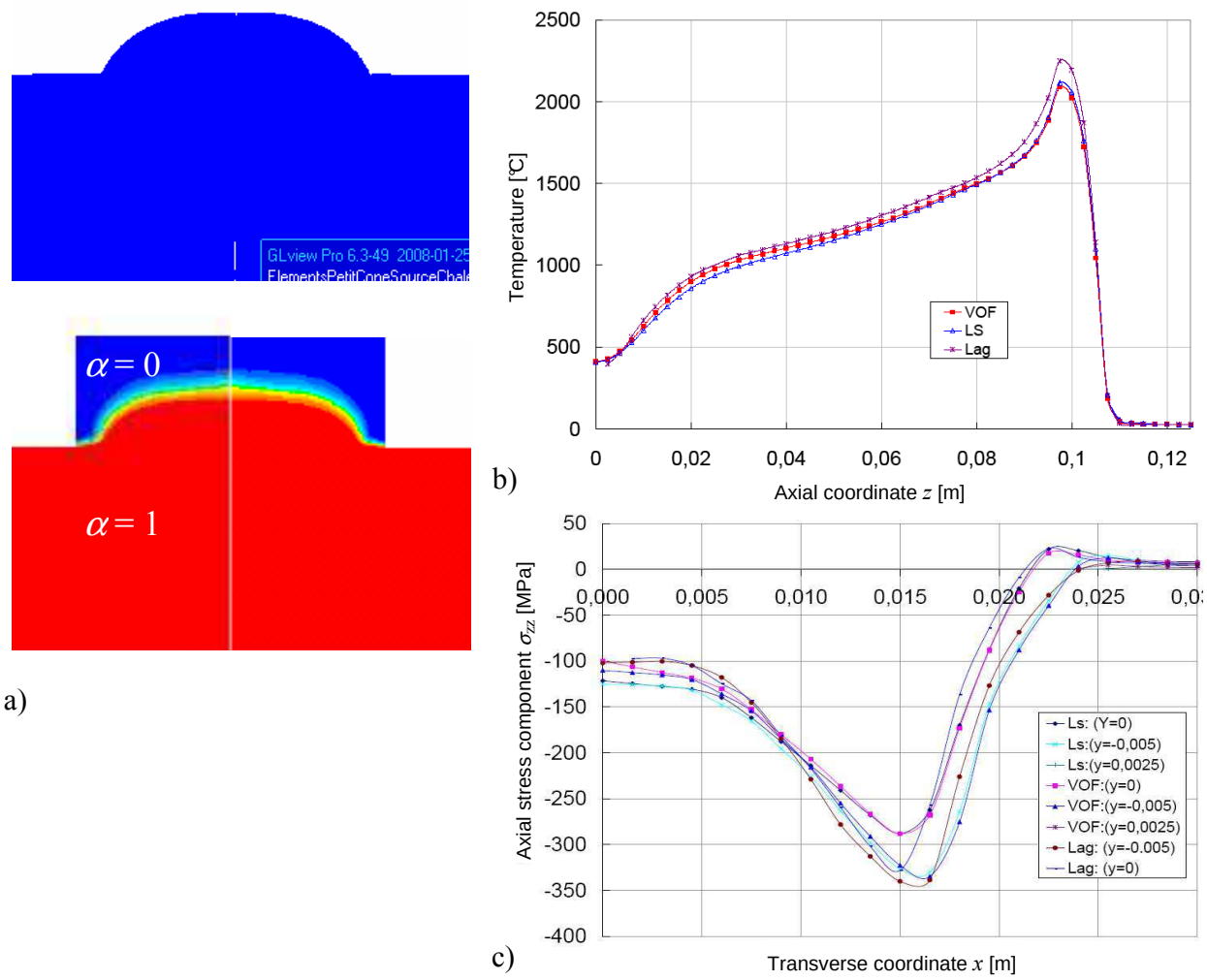

Figure 3. Comparison between Lagrangian and VOF-interface-tracking formulations. a) comparison of the shape of weld joint: using the Lagrangian method (top) and using the VOF method (bottom). b) Temperature profile along a centered axial line, at 1 mm below the surface of base metal. c) Axial stress profile along transverse lines at different depthes (y). Note that figures b) and c) include results from an alternative formulation (LevelSet, labelled LS [15]).

$$\|e\|_{\infty,K} \le c \max_{\mathbf{x}\in K} \max_{\mathbf{a}\in K} \left(\mathbf{a}\cdot|\mathbf{H}_u(\mathbf{x})|\mathbf{a}\right) \tag{14}$$

where $\mathbf{H}_u$ is the Hessian matrix of u (matrix of second spatial derivatives), $\mathbf{a}$ denotes the 6 edge vectors of the element and c is a constant. This relation means that denoting h_K the dimension of the element along one of the eigen directions of $\mathbf{H}_u$, of eigen value λ_K, the error in this direction varies like $h_K{}^2\lambda_K$. Assuming the linearity of the Hessian over the element $K = ABCD$ (which is the case, see hereunder), we obtain the following expression for the upper bound of the error:

$$\|e\|_{\infty,K} \le c \max_{\mathbf{a}\in K} \left(\mathbf{a}\cdot\overline{\mathbf{M}}\mathbf{a}\right) \quad \text{with} \quad \overline{\mathbf{M}} = \max_{P\in\{A,B,C,D\}} |\mathbf{H}_u(P)| \tag{15}$$

Taking this upper bound as an error estimation, it is then possible to obtain a uniform spatial distribution of a given accepted error ε, by checking that:

$$\forall K, \quad \forall \mathbf{a}\in K, \quad \varepsilon = c\left(\mathbf{a}\cdot\overline{\mathbf{M}}\mathbf{a}\right) \tag{16}$$

In other words, the mesh should be unitary for the metric $(c/\varepsilon)\overline{\mathbf{M}}$. The anisotropic remesher developed by Gruau & Coupez [14] is used to obtain this objective unitary mesh. The Hessian matrix is calculated at each node of the current mesh, using an approach based upon a local double L_2-projection, which is nothing but a nodal smoothing by an averaging weighted by the

volume of adjacent elements. In order to concurrently control the error of several fields of the finite element solution (temperature, stress, phase fraction), the metric associated to each field is calculated at each node, allowing the determination of a unique final objective metric to be provided to the remesher [3, 13, 15].

Inverse Modelling for Identification of Heat Sources

In thermal-metallurgical-mechanical modeling of welding processes, the physics governing the fluid flow in the weld pool is generally ignored. The reason lies in the high computation times it would need, because of the small length and time scales required by the numerical modeling of those phenomena (high speed Marangoni flow with electromagnetic coupling). Despite some efforts in that direction [15], it is difficult to envisage fully integrated numerical simulations before a couple of years. This is a real issue, since the thermal load determines the shape of the fusion zone, the heat affected zone and the stresses in the neighbourhood. The fluid flow being then ignored in such simplified simulations, its thermal effects are accounted for by means of a specific model for the energy supply. In the literature, a great variety of heat source models can be found. The use of augmented thermal conductivity, possibly anisotropic, is also frequent. In this context, we have applied an inverse analysis technique for the determination of the parameters governing the heat distribution and the magnification of the thermal conductivity.
The basic principle of the method is to adjust the values of the parameters in order to minimize the difference between numerical calculations and measurements. Given a characteristic experiment that is representative of some welding conditions (intensity, voltage, electrode height, filler supply conditions, geometry of configuration), the temperature is measured at specific locations and during a time interval, using for instance thermocouples. Denoting $T^{\exp}$ the measured temperatures and T^{cal} the calculated ones, a sampling procedure has to be defined in order that the vectors $\mathbf{T}^{\exp}$ and $\mathbf{T}^{\text{cal}}$ of T values can be compared. The calculated values T^{cal} of course depend on the set of parameters $\mathbf{q}$ and the distance is expressed in the sense of the classical least squares method. The inverse problem consists then in determining $\mathbf{q}$ such that the following function $\Psi(\mathbf{q})$ be minimized,

$$\Psi(\mathbf{q}) = \sum_{k=1}^{S}\sum_{i=1}^{I}(T_{k,i}^{cal}(\mathbf{q}) - T_{k,i}^{\exp})^2 \tag{17}$$

S denoting the number of sensors, k the sensor index, I the number of sampling instants, and i the index for sampling instants.
In a welding problem, the correct representation of the shape of the weld pool is important. With this in view, the function Ψ is complemented with additional terms such as Ψ_{FZ} and Ψ_{BM}, expressing that at locations where the metal was found melted in the experiment, the maximum of the calculated temperature should not be found below the liquidus temperature, and conversely, at locations where the metal was found not melted in the experiment, the maximum of the calculated temperature should not be found over the solidus temperature:

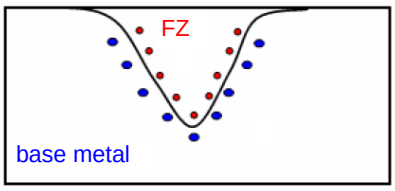

Figure 4. Schematics of the selection of locations in the fusion zone (FZ, in red) and in the base metal (in blue) in view of inverse analysis for heat source identification.

$$\Psi_{FZ}(\mathbf{q}) = \sum_{k=1}^{S_{FZ}}\left\langle T_L - \max_{i=1,I} T_{k,i}^{cal}(\mathbf{q})\right\rangle^2 \qquad \Psi_{BM}(\mathbf{q}) = \sum_{k=1}^{S_{BM}}\left\langle \max_{i=1,I} T_{k,i}^{cal}(\mathbf{q}) - T_S\right\rangle^2 \tag{18}$$

In these expressions, S_{FZ} denotes the number of selected locations in the fusion zone, and S_{BM} the number of selected locations in the non-melted base metal, according to the schematics of Figure 4. The expressions between brackets reduce to zero when negative : $\langle x\rangle = (x+|x|)/2$. The modified function that has been considered has the following expression,

$$\tilde{\Psi}(\mathbf{q}) = \frac{\beta}{S \times I} \sum_{k=1}^{S} \sum_{i=1}^{I} (T_{k,i}^{cal}(\mathbf{q}) - T_{k,i}^{\exp})^2 + (1-\beta)\left(\frac{1}{S_{FZ}} \sum_{k=1}^{S_{FZ}} \left\langle T_L - \max_{i=1,I} T_{k,i}^{cal}(\mathbf{q}) \right\rangle^2 + \frac{1}{S_{BM}} \sum_{k=1}^{S_{BM}} \left\langle \max_{i=1,I} T_{k,i}^{cal}(\mathbf{q}) - T_S \right\rangle^2 \right) \quad (19)$$

where β is a weighting factor.

The minimization problem is solved using the IOSO software [16]. Figure 5 gives an example of application of this identification method. The test case consists of a linear deposit using a GMA process. The material is a stainless steel 316L. Five parameters should be identified (vector **q**) are the followings: the overall welding heat efficiency η (fraction of power effectively transferred to the system), the magnification factor for heat conductivity f_k, the radius of the surface heat flux R_1, the surface thermal emissivity ε, the fraction of heat power transferred as a surface flux ω (the complement being transferred as a volume heat source, whose parameters can be determined following Kumar & DebRoy [17]). The optimization took 40 iterations (CPU time 96h on Pentium4 @ 2.8 GHz and 1Gb RAM), yielding the parameter values indicated in Table 1.

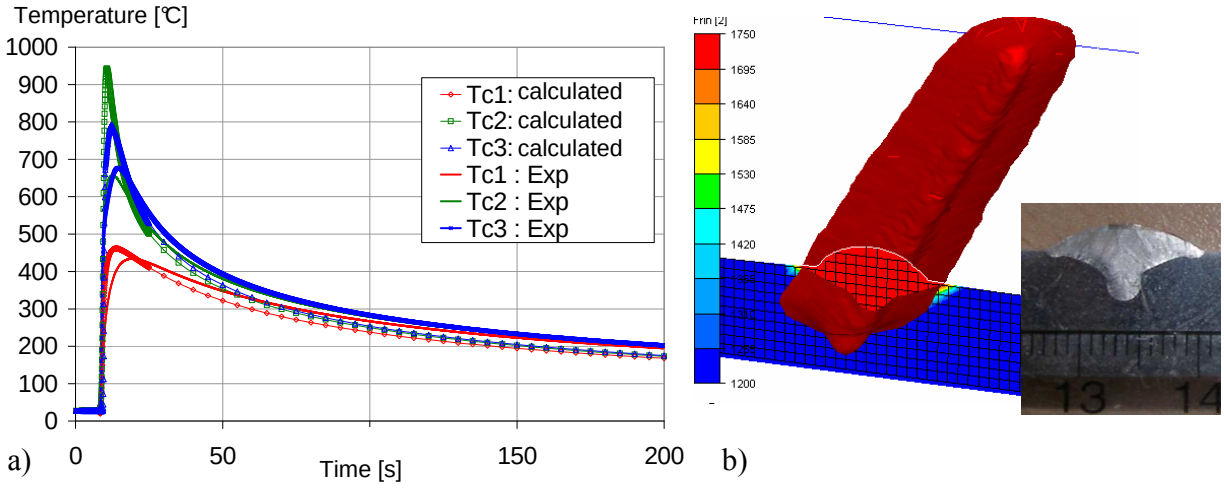

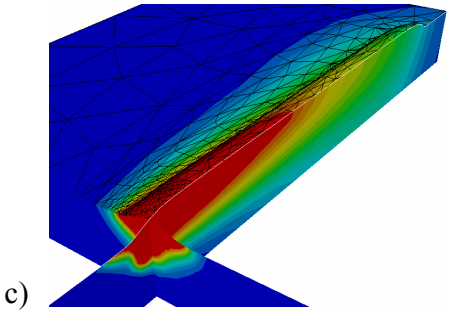

Figure 5. Application of the inverse analysis for identification of heat source in GMA welding of 316L stainless steel. a) Comparison between experimental and numerical temperature evolution at different selected locations, b) numerical transverse shape of fusion zone after identification process and experimental transverse shape of fusion zone, c) perspective view showing the shape of isotherms induced by the identified heat source.

η	f_k	R_1	ε	ω
0.85	20	8.5 mm	0.25	0.70

Table 1: values of heat source parameters issued from automatic identification.

Conclusions

Numerical methods have been developed with the objective of improving the capacities of arc welding simulation. Regarding material deposit and weld formation, the Lagrangian method is efficient when associated with adaptive remeshing. It provides a good and convenient alternative to classic element activation techniques, but is limited when simulating multipass and effective assembly of parts. Despite the need of meshing the air phase, the interface tracking method

offers significant advantages. Finally, the inverse finite element analysis is an efficient method to determine the welding energy input.

References

1. C. Pequet, P. Lasne, M. Hamide, E. Massoni, M. Bellet, "A coupled approach for the modelling of arc welding processes", Proc. 11th Int. Conf. on Modeling of Casting, Welding and Advanced Solidification Processes, Opio, C.A. Gandin, M. Bellet (eds.), The Minerals, Metals & Materials Society (2006) 855-862

2. M. Hamide, M. Bellet, "Adaptive mesh technique for coupled problems. Application to welding simulation", Proc. 9th Int. Conf. on Numerical Methods in Industrial Forming Processes, Porto, Portugal, American Institute of Physics (2007) 1561-1566

3. M. Hamide, E. Massoni, M. Bellet, "Adaptive mesh technique for thermal-metallurgical numerical simulation of arc welding processes", *Int. J. Num. Meth. Engng.* 73 (2008) 624-641

4. L.E. Lindgren, H. Runnemalm, M. Näsström, "Simulation of multipass welding of a thick plate", *Int. J. Num. Methods Eng.* 44 (1999) 1301-1316

5. J. Bruchon, "Etude de la formation d'une structure mousse par simulation directe de l'expansion de bulles dans une matrice liquide polymère", Ph.D. thesis, Mines-ParisTech (2004)

6. O. Basset, "Simulation numérique d'écoulements multi fluides sur grille de calcul", Ph.D. thesis, Mines-ParisTech (2006)

7. J.U. Brackbill, D.B. Kothe, C. Zemach, "A continuum method for modeling surface tension", *J. Comput. Physics* 100 (1992) 335-354

8. M. Bellet, "Implementation of surface tension with wall adhesion effects in a three-dimensional finite element model for fluid flow", *Comm. Num. Meth. Engng.* 17 (2001) 563-579

9. S. Gallot, D. Hulin, J. Lafontaine, *Riemannian Geometry*, Springer Verlag (2004)

10. S. Hysing, "A new implicit surface tension implementation for interfacial flows", *Int. J. Num. Meth. Engng.* 51 (2006) 659-672

11. M. Fortin, "Estimation d'erreur a posteriori et adaptation de maillages", *Revue Européenne des Eléments Finis* 9 (2000) 467-486

12. E. D'Azevedo, B. Simpson, "On optimal triangular meshes for minimizing the gradient error", *Numerische Mathematik* 59 (1991) 321-348

13. F. Alauzet, P. Frey, P. George, "Anisotropic mesh adaptation for Rayleigh-Taylor instabilities", Proc. ECCOMAS Congress on Computational Methods in Applied Sciences and Engineering 2004

14. C. Gruau, T. Coupez, "3D tetrahedral unstructured and anisotropic mesh generation with adaptation to natural and multidomain metric", *Comp. Meth. Appl. Mech. Eng.* 194 (2005) 4951–4976

15. M. Hamide, "Modélisation numérique du soudage à l'arc des aciers", Ph.D. thesis, Mines-ParisTech (2008)

16. I.N. Egorov, G.V. Kretinin, I.A. Leshchenko, S.V. Kuptzov, "Robust design optimization strategy of IOSO technology", 5th World Congress on Computational Mechanics, Vienna (2002)

17. A. Kumar, T. DebRoy, "Guaranteed fillet weld geometry from heat transfer model and multivariable optimization", *Int. J. Heat Mass Transfer* 47 (2004) 5793-5806

Acknowledgements

This study was supported by the companies Industeel (ArcelorMittal group) and Aubert et Duval.